Available online at www.sciencedirect.com
SCIENCE DIRECT®
Journal of the European Ceramic Society 25 (2005) 639–648
www.elsevier.com/locate/jeurceramsoc

Anisotropic X-ray diffraction peak broadening and twinning in diaspore-derived corundum

L. Löffler, W. Mader*

Institut für Anorganische Chemie, Universität Bonn, Römerstrasse 164, Bonn D 53117, Germany

Received 28 December 2003; accepted 6 March 2004
Available online 7 June 2004

Abstract

Corundum produced by dehydration of diaspore at temperatures between 400 and 1000 °C was studied by X-ray diffraction (XRD) and transmission electron microscopy (TEM). The broadening of XRD peaks and the size of corundum twin domains are related to the dehydration temperature. At low dehydration temperatures (<450 °C) as well as at high temperatures (>700 °C) large twin domains are obtained which yield sharp XRD peaks for all reflections. Dehydration between 450 and 600 °C leads to twin domains smaller than 10 nm. In this temperature range, significant peak broadening is observed, however, only for reflections, which structure factors are dominated by the aluminum sublattice and which are not common to both twin variants of corundum. The experimental results show that XRD peak broadening is only caused by fine twinning. Porosity in corundum as a reason for XRD peak broadening is excluded: the lamellar pore system is well ordered in corundum produced at low temperatures, however narrow peaks are observed. The reasons for the development of twin domains with differing sizes at different dehydration temperatures are discussed in detail.

Keywords: Dehydration; Al_2O_3; Twinning; X-ray diffraction; Electron microscopy

1. Introduction

Aluminum oxides and hydroxides are widespread in nature and of utmost industrial importance. Bauxites, aluminum ores containing different hydroxides and oxyhydroxides, are most important resources for the aluminum production, while the oxides are important ceramic materials. As initial step of all production, the thermal conversion of hydroxides into water-free, highly-porous oxides is very critical.

One of the reactions involved in this process is the dehydration of diaspore, α-AlOOH, which is the most stable aluminum oxide hydroxide. Whereas all other hydroxides and oxide hydroxides of aluminum dehydrate to metastable transition aluminum oxides diaspore (D) directly transforms to corundum (C), α-Al_2O_3 upon dehydration:

$$2AlO(OH) \rightarrow Al_2O_3 + H_2O.$$

The first study of that reaction revealed that the transformation is topotactic with the lattice planes $(1\,0\,0)_D \parallel (00.1)_C$ and $(0\,1\,0)_D \parallel (11.0)_C$.[1] The hexagonal stacking of close-packed oxygen layers, ABABAB, is preserved during the reaction. Hence, the dehydration reaction requires only short range cationic rearrangement. From the reaction equation, however, it follows that a quarter of the oxygen atoms is removed during dehydration. This loss of oxygen atoms (and hydrogen) is accompanied by the formation of pores in the dehydration product.[2] In a more recent study, it has been shown that at low temperature (400 °C) dehydration of diaspore the pores are two-dimensionally aligned in lamellae parallel to the basal plane in the product, and the lamellae appear periodically at a distance of approximately 3.7 nm.[3] Dehydration at higher temperatures gradually degenerates the uniform pore structure. It has been shown that these pores act as diffusion paths for the water molecules to escape from the system during the reaction. Hence, the anisotropy of the dehydration of diaspore crystals can be understood considering the geometry of pores, cracks and cleavage planes.[3]

The subject of the present paper is the anisotropic peak broadening in powder X-ray diffraction (XRD) measurements of the dehydration product. This characteristic phenomenon has rarely been studied for diaspore-derived corundum,[2,4] where authors discussed XRD results without

* Corresponding author.
E-mail address: mader@uni-bonn.de (W. Mader).

0955-2219/$ – see front matter © 2004 Published by Elsevier Ltd.
doi:10.1016/j.jeurceramsoc.2004.03.027

Table 1
Heat treatment (temperature and time) of powder samples and single crystal specimens

Dehydration temperature (°C)	Powder (for XRD)	Single crystals (for TEM)
400	–	28 days[a]
410	50 days	–
430	2 days	1 day[a]
445	30 h	–
460	20 h	
500	–	90 min[a]
525	1 h	–
550	–	30 min[a]
600	1 h	3 min[a]
650	1 h	–
700	1 h	1 h
800	1 h	1 h
1000	1 h	1 h

[a] Only partial transformation.

further TEM investigation. However, for the analogous dehydration reaction in the iron oxide system—goethite (α-FeOOH) to hematite (α-Fe_2O_3)—a number of investigations have been reported over the past decades. In both systems, the diffraction peaks of the types (01.2), (10.4), (11.6), (02.4), (01.8) and (21.4) are significantly broadened compared to the (11.0), (11.3) and (30.0) reflections. So far, the anisotropic broadening has been observed exclusively in low-temperature dehydration products, e.g. for goethite-derived hematite at temperatures lower than 600 °C. Regarding these previous studies, two different approaches have been made to explain that phenomenon: One refers to the crystal shape anisotropy due to the pore lamellae,[5–10] while the other ascribes the broadening to cationic disorder, caused by either very fine twinning[11–14] (domain sizes of about 5 nm) or residual hydroxyl groups.[15–17]

Up to now, for both of these interpretations series of papers have been published on the goethite/hematite system, however, no agreement has been achieved yet. In the present study, XRD peak broadening of diaspore-derived corundum as a function of dehydration temperature has been examined in direct correlation with high resolution and dark field TEM studies on twinning—an investigation which has not been performed so far. The results of the combined XRD and TEM study will be discussed with respect to the crystal structure and the microstructure of the dehydration product. In addition, high angle reflections in X-ray powder scans will be considered which provide further information and support for the interpretation given in the present paper. Finally, we shall be able to explain the anisotropic peak broadening with fairly simple arguments.

2. Experimental

All studies were performed on dehydration products of natural gem-quality diaspore from the Menderes region, Turkey. For the XRD measurements, parts of the crystal were crushed to a fine powder before heating. For the different reaction temperatures, the reaction time was chosen as listed in Table 1. The samples were directly placed into the hot tube furnace, and were quickly removed after the reaction time. This was done to avoid modification of the product by the heating or cooling procedure. In any of the thermal treatments listed in Table 1 complete conversion to corundum was achieved.

Natural diaspore powder consists of (0 1 0) plate-shaped crystals. To avoid falsification of intensity due to the (0 1 0) texture the X-ray diffraction intensities were acquired in Debye–Scherrer geometry. The data were collected on a STOE diffractometer, Stadi P (Cu Kα radiation), equipped with a position sensitive detector (PSD, 0.03° angular resolution). The XRD scans were evaluated using DIFFRAKT 97, which allows profile fitting with high accuracy for each of the reflections separately.

For TEM studies the diaspore crystals were cut into blocks with dimension of 6 mm × 1.8 mm × 0.3 mm, where cutting was performed along all principal planes of diaspore, respectively. The samples were annealed in air at temperatures ranging from 400 to 1000 °C for different times, which led to partial or total transformation to corundum (see Table 2). Again, the samples were directly placed into the hot tube furnace and were quickly removed and cooled down by dropping them on a cold metal plate. The oriented TEM specimens were prepared in cross-section using common procedures for TEM specimen preparation. The TEM studies were performed on electron microscopes type Philips CM30ST and type Philips CM300UT, both operated at 300 kV.

Table 2
Size and shape of twin domains as function of dehydration temperature

Dehydration temperature (°C)	Size of twin domains (along × normal to basal plane)	Shape	Twin boundary plane
400	1 μm × 200 nm	Elongation ‖ (0 0 0 1)	Favorably (0 0 0 1)
430	100 nm × 40 nm	Elongation ‖ (0 0 0 1), less pronounced	Still favorably (0 0 0 1)
500–600	10 nm × 10 nm	Random	Random
800	40 nm × 100 nm	Elongation ‖ ($\bar{1}$ 1 0 0)	Favorably ($\bar{1}$ 1 0 0)
1000	100 nm × 300 nm	Elongation ‖ ($\bar{1}$ 1 0 0), less pronounced	Favorably ($\bar{1}$ 1 0 0)

3. Results

3.1. X-ray diffraction

XRD scans between 15° and 95° 2θ were acquired on diaspore-derived corundum produced at different dehydration temperatures ranging from 410 to 1000 °C. A list of four of these scans (410, 600, 700 and 1000 °C) are displayed in Fig. 1 for a direct comparison. The full width at half maximum (FWHM), representing the XRD peak width, of prominent reflections are plotted against the dehydration temperature in Fig. 2a. The accuracy in the FWHM values was determined by multiple fitting to be approximately 0.015°. Since the peak widths depend on the Bragg angle by $1/\cos\theta$, in Fig. 2b they are plotted in terms of FWHM $\cos\theta$ against dehydration temperature for better comparison of different reflections. As can be seen from Fig. 2, the change in peak width as a function of temperature strongly depends on the individual reflection.

Two groups of reflections may be distinguished. Group I reflections consist of (11.0), (11.3) and (30.0) showing small (approximately 0.2°) and virtually constant peak widths for all temperatures examined. The (11.6) reflection is close to the group I reflections and exhibits a moderate increase (less than 0.05°) in peak width.

Somewhat striking is the course of the peak widths of the group II peaks which are represented by the reflections of type (01.2), (10.4), (02.4) and (21.4) in Fig. 2. At dehydration temperatures below 450 °C the peak widths are between 0.22° and 0.27°. Above 450 °C, however, the widths abruptly increase to 0.4°–0.55° (twice the values at lower temperature), and the widths remain at these large values up to 600 °C. At even higher temperatures, the group II peak widths decrease continuously approaching the values at lowest dehydration temperature at 1000 °C. The latter phenomenon, the sharpening of the XRD peaks with increasing temperature, has been observed previously—almost exclusively for the goethite/hematite system. However, to our knowledge the narrow XRD peaks after low temperature dehydration have never been reported before.

3.2. TEM observations

Cationic disorder such as twinning is an origin for diffraction peak broadening. Since twinning of the dehydration product is of particular interest it shall be described in more detail.

The corundum structure is based on a hexagonal stacking of close-packed oxygen layers (...ABAB...), where two thirds of the octahedral sites (γ) are occupied with aluminum forming a "honeycomb" pattern. From one layer to the next, only the positions of the empty octahedral sites are shifted in such a way that the stacking sequence repeats every third layer. The resulting aluminum layers may be denoted as γ, γ' and γ''.

In diaspore, the repeating sequence of the cation stacking comprises two layers. Therefore, the dehydration of diaspore is associated with a change in symmetry along the direction of closed packing either from 2_1 to 3_1 or from 2_1 to 3_2, resulting in two possible different stacking sequences of the dehydration product, i.e.

$$\mathrm{A}\,\gamma\,\mathrm{B}\,\gamma'\,\mathrm{A}\,\gamma''\,\mathrm{B}\,\gamma\,\mathrm{A}\,\gamma'\,\mathrm{B}\,\gamma'' \quad (1)$$

or

$$\mathrm{A}\,\gamma\,\mathrm{B}\,\gamma''\,\mathrm{A}\,\gamma'\,\mathrm{B}\,\gamma\,\mathrm{A}\,\gamma''\,\mathrm{B}\,\gamma'. \quad (2)$$

The two stacking sequences represent two twin variants of corundum and may be denoted as "obverse" (1) and "reverse" (2).[18] Therefore, the corundum derived from diaspore must be twinned containing the two twin variants in equal amounts, and the microstructure consists of twin

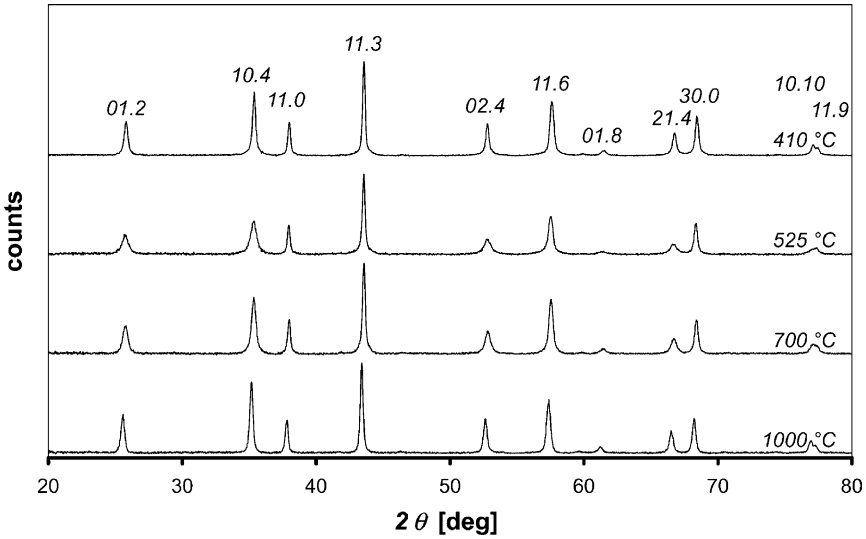

Fig. 1. XRD scans of the corundum powders obtained from crushed natural diaspore samples after dehydration at 410, 525, 700 and 1000 °C.

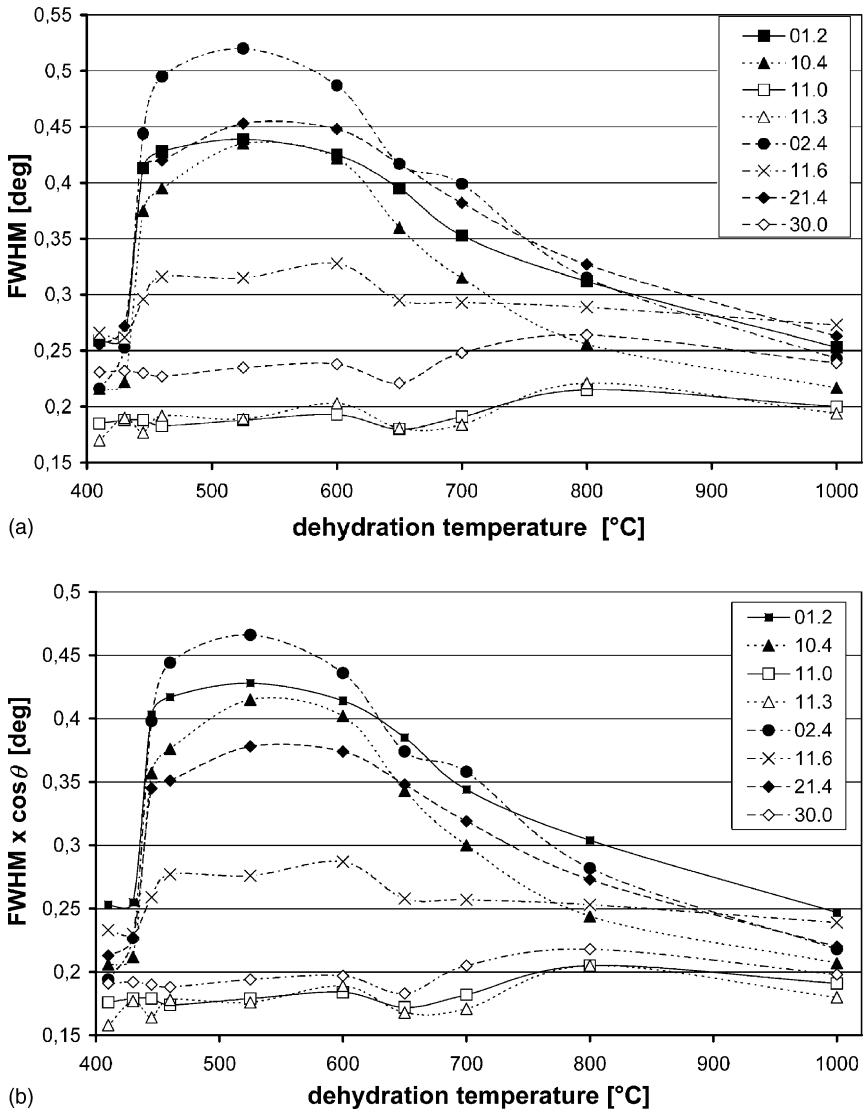

Fig. 2. (a) Full width at half maximum (FWHM) height of eight dominant corundum reflections obtained from diaspore as a function of dehydration temperature. (b) Representation of the widths of diffraction peaks in (a) as FWHM $\cos\theta$ plotted against the dehydration temperature.

domains. By means of TEM, twinning in corundum can be viewed most readily along the *a*-axis,[19] e.g. along the $[1|1|\bar{2}|0]$ direction. Both the structure as well as the diffraction patterns of the twin variants can be transformed into each other by a mirror operation at the basal plane. Consequently, $[0\,0\,0\,1]_{\mathrm{I}}$ direction of twin variant one points in the direction of $[0|0|0|\bar{1}]_{\mathrm{II}}$. In the following, the two variants are indexed I (obverse) and II (reverse).

The size and the shape of the twin domains were characterized using dark field and high resolution imaging along the $[1|1|\bar{2}|0]$ direction, a diffraction pattern of twinned corundum crystals is shown in Fig. 3. The reflections $(2|\bar{2}|0|4)_{\mathrm{I}}$ and $(1|\bar{1}|0|\bar{4})_{\mathrm{II}}$ were used for the dark field images presented here. Thus, the two twin variants could be separately imaged and sized. Fig. 4a and b represents dark field images of a sample dehydrated at 400 °C. The twin domains amount to several 100 nm, in some cases they are more than 1 μm in size. Average values of twin domain sizes are given in Table 2. The twin boundaries are predominantly parallel to (0 0 0 1) forming basal twins and the twin domains are elongated along the basal plane. The speckle variation in image contrast within one twin domain is caused by the pore lamellae as discussed in detail elsewhere.[3] Fig. 4a and b may be directly compared to the pair of images in Fig. 5a and b, which are from a specimen dehydrated at 600 °C. The twin domains are very small and their size cannot be determined via dark field imaging. No typical shapes or twin boundaries can be detected (cf. Table 2). Additional high resolution imaging was necessary for this purpose as will be shown below. At 800 °C the average size of twin domains is again larger, approximately 40 nm × 100 nm (Fig. 6). However, the shape of the domains has changed compared to the ones in the 400 °C samples. At higher temperature the $\{0\,0\,0\,1\}$ faces are smaller than the $\{\bar{1}|1|0|0\}$ faces. Additionally, the

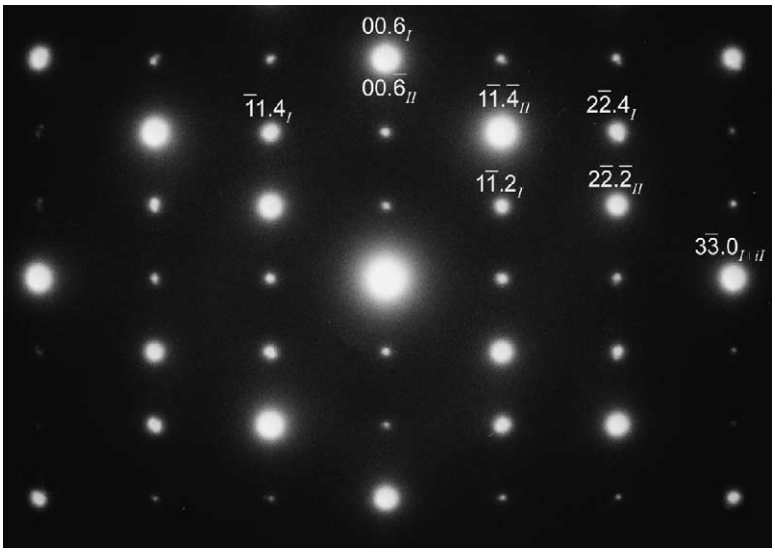

Fig. 3. Electron diffraction pattern of twinned corundum in [2|1̄|1̄|0]: reflections such as (00.6) and (3̄3.0) of the twin variants I and II coincide while other reflections belong to one variant only.

pore lamellae have coagulated to almost spherical pores. After dehydration at 1000 °C (Fig. 7), the average domain size has further increased to some few 100 nm. The twin domains are more irregularly shaped than in the 800 °C samples. However, the {1̄|1|0|0} twin boundaries are still prevailing.

High resolution imaging was performed on the dehydration products along the same crystal axis, [1|1|2̄|0]. The

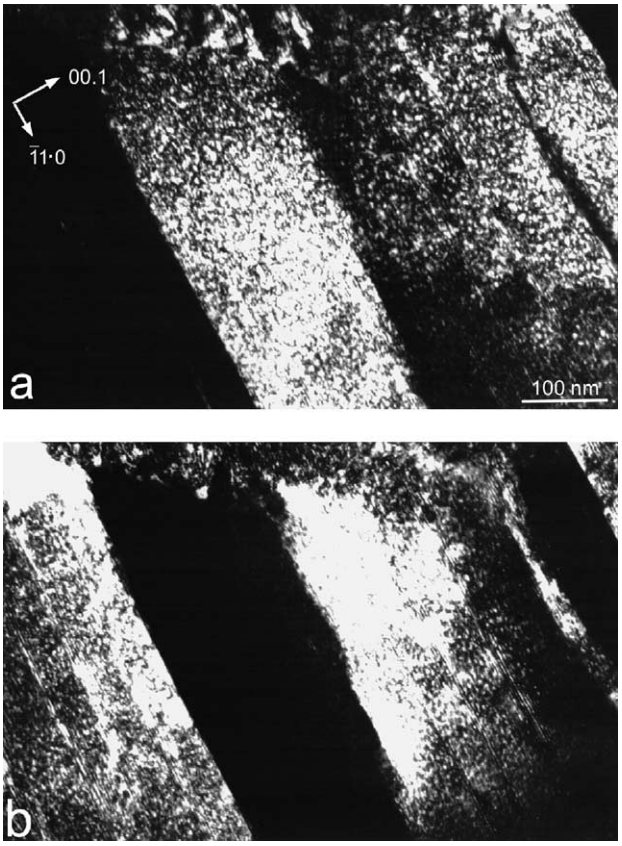

Fig. 4. TEM dark field images of twinned corundum produced by dehydration at 400 °C. (a) Image taken with $(\bar{1}1.4)_{I}$, (b) image taken with $(2\bar{2}.4)_{II}$. The contrast in the image pair is complementary: one variant appears bright while the other variant remains dark.

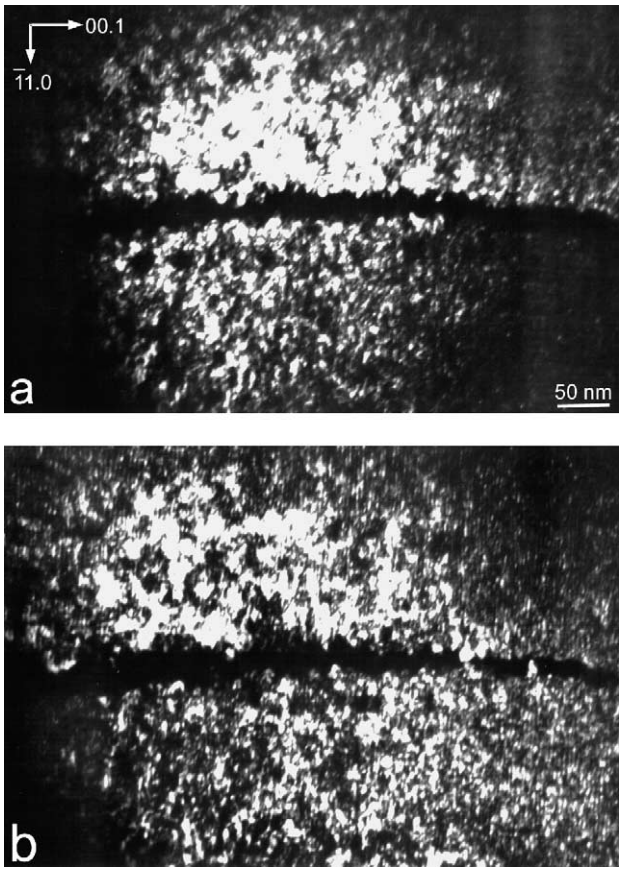

Fig. 5. TEM dark field image pair of twinned corundum produced by dehydration at 600 °C. Images (a) and (b) taken with the reflections used for Fig. 4.

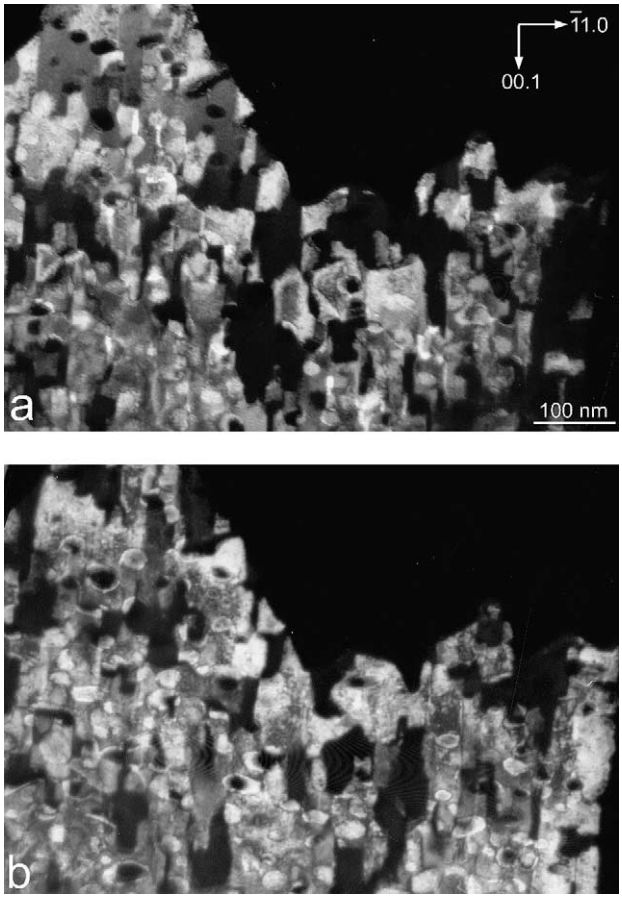

Fig. 6. TEM dark field image pair of twinned corundum produced by dehydration at 800 °C. Images (a) and (b) taken with the reflections used for Fig. 4.

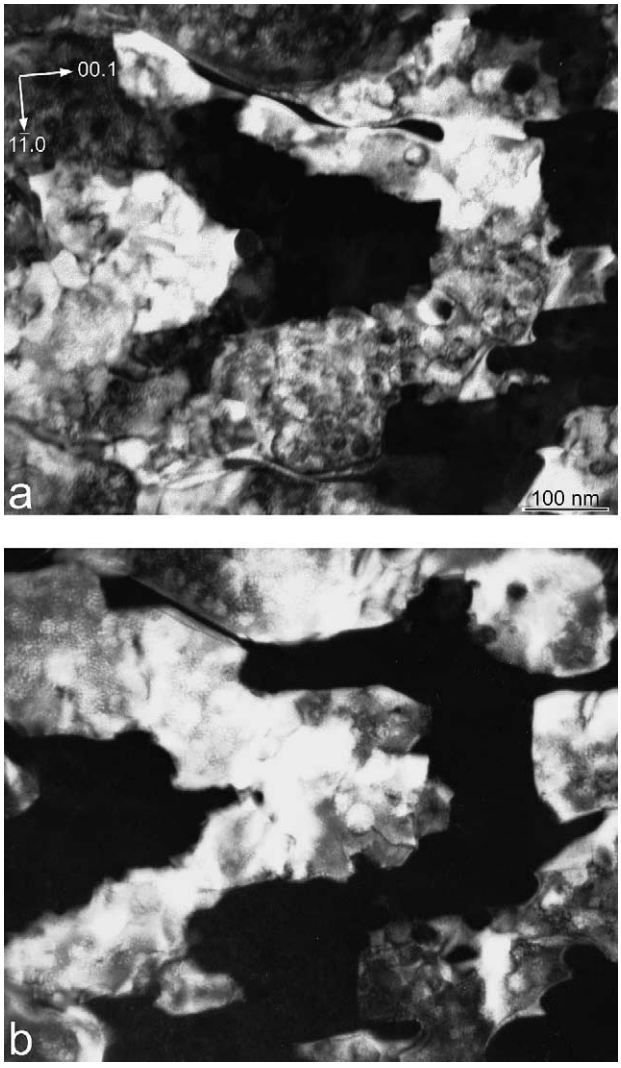

Fig. 7. TEM dark field image pair of twinned corundum produced by dehydration at 1000 °C. Images (a) and (b) taken with the reflections used for Fig. 4.

lattice image of corundum produced at 600 °C is shown in Fig. 8, wherein both the $(1\bar{1}.2)_{\mathrm{I}}$ and the mirror-related $(1\bar{1}.2)_{\mathrm{II}}$ lattice fringes of the two variants are resolved. In regions where the two variants overlap due to projection, $\{0\,0\,0\,2\}$ and $\{\bar{1}|1|0|0\}$ fringes are produced, which are not common to corundum. Their appearance has been explained by Watari et al.[11] on dehydrated goethite comparing HRTEM images to the projected atomic structure of an overlapping twin. Thus, the additional fringes in the HRTEM image are to be regarded as a Moiré contrast of overlapping crystals in twin orientation. In Fig. 8, a number of these Moiré patterns are observed. The exact orientation of the twin domain boundaries cannot be resolved, however, any overlapping region in the thin foil has to contain at least one domain boundary. Therefore, the average size of the twin domains can be estimated to lie between 5 and 10 nm.

4. Discussion

4.1. Non-uniform peak broadening and structure factors

From the observations described above, it emerges that twinning and the twin sizes in corundum are strongly related to the anisotropic XRD peak broadening of some of the X-ray reflections. Since twinning only affects the aluminum sublattice—while the oxygen sublattice continuous over both twin variants—it is worth sorting the reflections into groups dominated either by the aluminum or by the oxygen sublattice of corundum. This can be done by relating the peak width to its structure factors squared, F^2_{hkl}. The values are listed for Cu Kα radiation in Table 3. This table also contains the squared structure factors of the aluminum sublattice $F^2_{hkl}(\mathrm{Al})$ and of the oxygen sublattice $F^2_{hkl}(\mathrm{O})$ of corundum, respectively. Additionally, the contribution of the two sublattices to individual reflections is visualized in Fig. 9, where calculated powder diffraction scans of corundum and its oxygen and aluminum sublattice are displayed, respectively.

(i) The group I reflections (sharp peaks) are either reflections of type (*hk*.0) or their structure factor is dominated

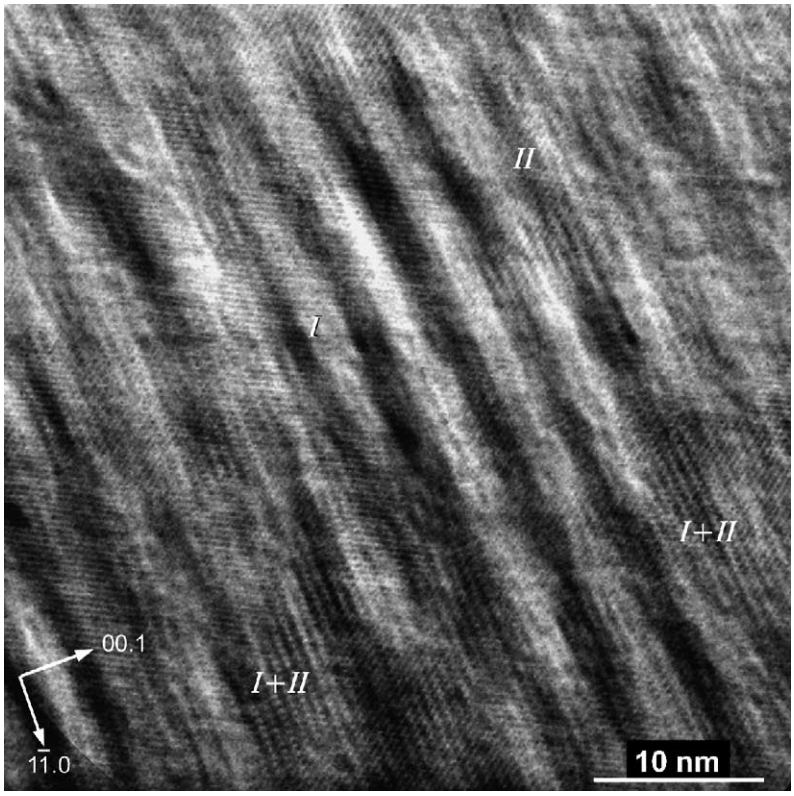

Fig. 8. High resolution TEM image in $[2|\bar{1}|\bar{1}|0]$ of twinned corundum produced by dehydration at 600 °C. Three different types of regions can be distinguished: (i) $(1\bar{1}.2)_{\mathrm{I}}$ lattice fringes of variant I resolved, (ii) $(1\bar{1}.2)_{\mathrm{II}}$ lattice fringes of variant II resolved, and (iii) regions where forbidden (00.2) fringes and $(1\bar{1}.0)$ fringes are observed due to double diffraction from overlapping twin variants I + II.

by the oxygen ions. The latter can be explained by the stacking sequence of the corundum structure, where the periodicity length of the stacking of the oxygen layers is one third of the length of the *c*-axis (=*c*/3). Hence, the reflections indexed (*hk*.3*n*), n = odd, are exclusively caused by the oxygen sublattice of corundum, i.e. $F_{hkl}^{\mathrm{Al}} = 0$. This is the case for the (11.3) reflection.

(ii) The group II reflections (broad peaks) are of the type (*hk*.2*n*) with $n \neq$ multiple of 3. It can be seen from Table 3 that the structure factors of these reflections are throughout dominated by the aluminium ions. This can be understood considering the periodicity of the stacking of the aluminium layers in corundum, which is half the length of the *c*-axis (=*c*/2).

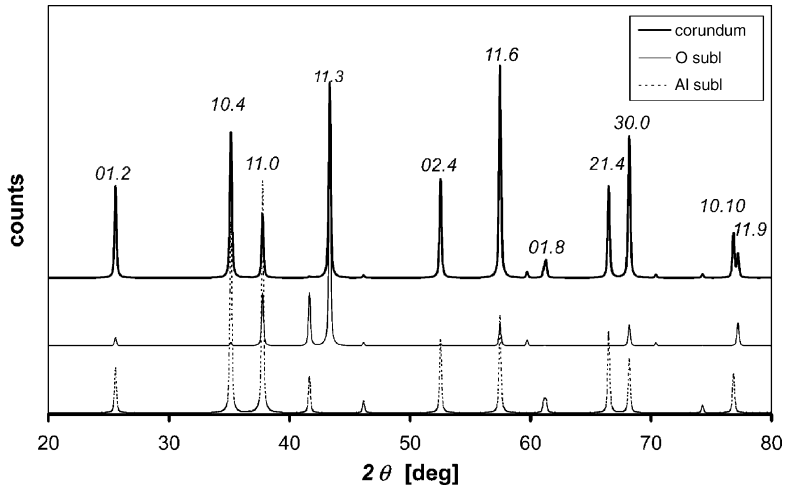

Fig. 9. Simulated XRD scans: corundum structure (top), oxygen sublattice of corundum (center), and aluminum sublattice of corundum (bottom).

Table 3
Lattice plane spacings (d), 2θ angles and calculated structure factors F^2_{hkl} for α-Al_2O_3, for the Al sublattice and for the O sublattice of corundum for each of the eight dominant corundum reflections, respectively

hkl	*d* (Å)	2θ (°) Cu Kα	F^2_{hkl}(Al) (e^2)	F^2_{hkl}(Al) (e^2)	F^2_{hkl}(O) (e^2)
01.2	3.477	25.60	9.76	7.24	2.52
10.4	2.549	35.18	17.23	19.39	2.16
11.0	2.377	37.82	12.75	22.48	9.73
11.3	2.083	43.40	15.34	0	15.34
02.4	1.738	52.60	19.23	16.54	2.69
11.6	1.600	57.55	21.12	14.26	6.86
21.4	1.403	66.59	15.61	14.65	0.96
03.0	1.372	68.20	28.02	17.17	10.85

(iii) The structure factor of reflections indexed (*hk*.3*n*), n = even, are originated from both the aluminium sublattice and the oxygen sublattice (cf. Table 3). The (11.6) reflection is of that type, and its peak width lies in between that of the two groups of reflections.

The reflections of type (*hk*.0) have to be discussed with respect to the twinning of corundum. Twinning is realized by a mirror operation at the basal plane. Therefore, the (*hk*.0) type reflections are not affected by twinning as they are twin invariant reflections common to both of the two twin variants. This is visualized in the diffraction pattern in Fig. 3, where the reflections of type (30.0) coincide in the diffraction patterns of both twin variants. For this type of reflections, it does not matter which type of sublattice dominates the structure factor.

The above considerations may be related to the TEM observations on the microstructure of the dehydration product. For large twin domains produced at very low or at very high dehydration temperatures all diffraction peaks show a regular small width. As shown in the results of XRD and TEM, the broadening of the peaks is definitely connected with the twin size: the smaller the twin size the broader are some of the corundum reflections. A further and strong argument is provided by the type of reflections which are broadened. Broadening is exclusively observed for reflections which are affected by twinning. These are exclusively reflections with structure factors dominated by the aluminum sublattice, and twinning of corundum only concerns the aluminum sublattice.

The non-uniform X-ray peak broadening in goethite-derived hematite has been the subject of debate from the 1950s of the past century to the latest literature. Models which try to explain that phenomenon by porosity and the plate-like appearance of the dehydration product can be found even in recent studies (see, e.g. Ref. 9). However, this cannot be the origin for that phenomenon: it is clearly shown from our results that the smallest peak widths are observed in XRD on the low temperature dehydration product where the pores are very regularly aligned and resemble a plate-like microstructure.[3] At first glance our observations seem to be inconsistent, because satellites and diffuse intensity around reflections have been observed in single crystal X-ray diffraction[2] and even more clearly in electron diffraction patterns of hematite[18] and of corundum.[2,3] These phenomena have been doubtlessly ascribed to the lamellae formed within the dehydration products. However, diffraction from single crystals is dynamic, i.e. multiple scattering of the beam takes place. This is in principle always true for electron diffraction and for X-ray diffraction from large crystals. In the dynamic case intensity of reflection $\vec{g}_1$ may be diffracted again, e.g. at lattice planes $\vec{g}_2$ producing another reflection at $\vec{g}_3 = \vec{g}_1 + \vec{g}_2$ by double diffraction realized by vector addition. In the dehydration product, the regular array of pores first produce satellite spots round the primary beam by single scattering processes. The satellites are then transferred to any other regular reflection of the crystal by double diffraction. As a result, practically all reflections of the crystal are surrounded by satellites (see, e.g. Ref. 3). However, the crystals in powder X-ray diffraction are too small to cause double diffraction of X-rays. Hence the array of pores produces satellites round the primary beam which could be detected in the low angle regime but not in a common X-ray powder pattern. In an excellent paper Lima-de-Faria[2] has already stated in 1963 that "*the non-uniform broadening of the powder peaks seemed to be a different effect to the satellites and diffuse regions*," and that it is "*essential to specify the size and texture of the material used*," to which we fully agree. Hence, the non-uniform broadening of X-ray powder peaks can be definitely related to the twinning of the dehydration product of diaspore (or hematite) as already proposed by Watari et al.[4]

In our discussion we shall also consider reflections of the type (10.10) and (11.9) in the high angle 2θ regime of the XRD scans (see Fig. 2). The peak widths of these reflections have never been discussed in the literature, however they contain important information which clearly support our interpretation. The reflections are ideal for a comparison since they appear at similar Bragg angles and their inclination to the basal plane is low, i.e. they would be similarly affected by the porous lamellae. In Fig. 10, their peak widths are plotted against the dehydration temperature. Their peak widths are much more difficult to measure since they overlap and are of low intensity. The error of each peak width was estimated by (a) multiple fitting and (b) an intensity factor, and the error is given by the bars in Fig. 10. In spite of all difficulties it is evident that the (10.10) reflection is broadened and belongs to the group II reflections, while (11.9) shows almost constant peak widths over the whole temperature range as it is expected for a reflection which is purely originated by oxygen. From these two reflections whose only essential difference is the type of the dominating sublattice, further evidence is provided that the twin-related disorder in the aluminum sublattice is the only reason for the peak broadening.

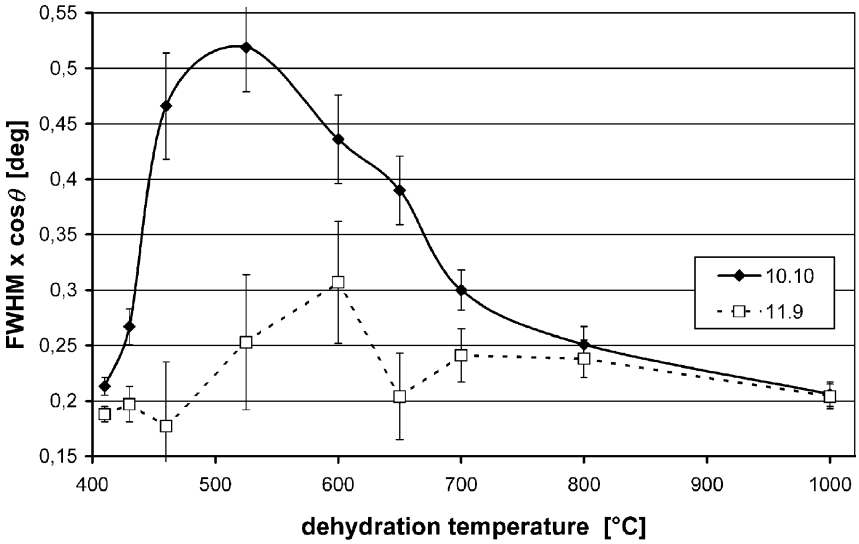

Fig. 10. FWHM $\cos\theta$ of (10.10) and (11.9) corundum reflections plotted vs. the dehydration temperature. Relatively large errors occur due to low count rates and partial overlap of the peaks.

4.2. Generation of twins by nucleation and growth

The relation between twin domain sizes and dehydration temperature may be explained by kinetic and thermodynamic aspects responsible for the generation of the twin microstructure, which is basically nucleation and growth of twin domains.

At temperatures below 430 °C, the transformation is very slow, which is especially true for the nucleation process. Very few corundum nuclei are formed—almost exclusively at the diaspore/air interface on the outer and inner surface (cracks) of the crystal. Once a nucleus of corundum has formed it gradually grows to a large domain by attaching Al^{3+} and O^{2-} species supplied by the dehydration process.[20] Hence, twin domains in the corundum will only occur if two neighboring nuclei are in twin orientation. This scenario is supported by the observation that (00.1) oriented twin boundaries in the corundum are clearly favored at low temperature (see Fig. 4). Two reasons are responsible for that: first, the dehydration along $[0\,1\,0]_D$ and $[0\,0\,1]_D$ was found to be much faster than along $[1\,0\,0]_D$,[3] which means that growth parallel to the basal plane of corundum is preferred. Second, twin faces are favorably produced in regions of low density, i.e. in the pore lamellae, which reduces the free energy of the system. From the width of the twin domains in Fig. 4 it is even possible to estimate the spacing of corundum nuclei to 50–100 nm.

At temperatures exceeding 450 °C, the thermodynamic driving force for the formation of corundum is increased. Due to the enhanced decomposition rate of diaspore a crystallographically less ordered product is formed. This is equivalent to the formation of a large number of nuclei at the diaspore–corundum interface. Again, nuclei of both twin variants are produced in equal amounts, and a finely twinned dehydration product is obtained. Obviously, at temperatures below 600 °C the twin domains do not coarsen, and the finely twinned microstructure originated at the reaction interface is preserved throughout the dehydration product (Fig. 5). This microstructure with very small twin domains is the reason for broadening of XRD peaks.

Above 600 °C, coarsening is clearly observed in the TEM images by a continuous increase of the twin domain sizes. This is the result of thermally induced ordering of the aluminum ions. At these higher temperatures, $\{\bar{1}|1|0|0\}$ twin boundaries along prism planes are preferred, which may be explained by thermodynamically controlled growth of twin domains (Fig. 6). At 1000 °C, coarsening of grains may take place so rapidly that no preferred twin boundary planes are detected (Fig. 7). The resulting microstructure with large twin domains does not produce broadening of XRD peaks as observed in XRD scans.

5. Conclusion

Corundum produced by dehydration of diaspore at temperatures between 400 and 1000 °C was studied by XRD and TEM. The broadening of XRD peaks and the size of corundum twin domains is a function of dehydration temperature, and a clear correlation exists between the peak width and the twin domain size.

(i) At low dehydration temperature (<450 °C) narrow XRD peaks and large twin domains are observed. Large twin domains are formed by kinetically controlled processes, where diaspore decomposition takes place slowly so that all atoms are attached to the existing corundum structure at perfect sites. Almost no new twin domains are formed at the phase boundary. Because the lamellar pore system in corundum is

ordered best in this temperature range we conclude that porosity is not the reason for peak broadening.

(ii) At the medium dehydration temperature range (450–600 °C), the number of new nuclei at the phase boundary is drastically increased. Thus, only small twin domains develop and broadening of aluminium-dominated reflections is observed. Since twinning is the only phenomenon to exclusively affect the aluminum sublattice, XRD peak broadening of diaspore-derived corundum is concluded to be caused by fine twinning only.

(iii) At higher dehydration temperature, thermodynamically controlled coarsening of twin domains results in larger domain sizes, and with increasing dehydration temperature all XRD peaks continuously sharpen, until at 1000 °C, the peaks are almost as sharp as after 410 °C dehydration.

Acknowledgements

The authors would like to thank Dr. Adelheid Niesert for her helpful assistance with the XRD measurements.

References

1. Deflandré, M., La structure cristalline du diaspore. *Bull. Soc. Franc. de Minéral.* 1932, **55**, 140–165.
2. Lima-de-Faria, J., Dehydration of goethite and diaspore. *Z. Krist.* 1963, **119**, 176–203.
3. Löffler, L. and Mader, W., Electron microscopic study of the dehydration of diaspore. *Am. Miner.* 2001, **86**, 293–303.
4. Watari, F., van Landuyt, J., Delavignette, P., Amelinckx, S. and Igata, N., X-ray peak broadening as a result of twin formation in some oxides derived by dehydration. *Phys. Stat. Sol.* 1982, **73**, 215–224.
5. Naono, H. and Fujiwara, R., Micropore formation due to thermal decomposition of acicular microcrystals of α-FeOOH. *J. Colloid Interface Sci.* 1980, **73**, 406–415.
6. Duvigneaud, P. H. and Derie, R., Shape effects on crystallite size distributions in synthetic hematites from X-ray line-profile analysis. *J. Solid State Chem.* 1980, **34**, 323–333.
7. Naono, H., Nakai, K., Sueyoshi, T. and Yagi, H., Porous texture in hematite derived from goethite: mechanism of thermal decomposition of goethite. *J. Colloid Interface Sci.* 1987, **120**, 439–450.
8. Hirokawa, S., Naito, T. and Yamaguchi, T., Effect of atmosphere on the goethite decomposition and pore structure of product particles. *J. Colloid Interface Sci.* 1986, **112**, 268–273.
9. Jiang, J. Z., Stahl, K., Nielsen, K. and da Costa, G. M., Anisotropic X-ray line broadening in goethite-derived haematite. *J. Phys. Condens. Matter* 2000, **12**, 4893–4898.
10. Perez-Maqueda, L. A., Criado, J. M., Real, C., Subrt, J. and Bohacek, J., The use of constant rate thermal analysis (CRTA) for controlling the texture of hematite obtained from the termal decomposition of goethite. *J. Mater. Chem.* 1999, **9**, 1839–1845.
11. Watari, F., van Landuyt, J., Delavignette, P. and Amelinckx, S., Electron microscopic study of dehydration transformations. I. Twin formation and mosaic structure in hematite derived from goethite. *J. Solid State Chem.* 1979, **29**, 137–150.
12. Goss, C. J., The kinetics and reaction mechanism of the goethite to hematite transformation. *Mineral. Mag.* 1987, **51**, 437–451.
13. Pomiès, M.P., Morin, G. and Vignaud, C., XRD study of the goethite-hematite transformation: application to the identification of heated prehistoric pigments. *Eur. J. Solid State Inorg. Chem.* 1998, **35**, 9–25.
14. Pomiès, M.P. and Menu, M., Vignaud, TEM observations of goethite dehydration: application to archaeological samples. *J. Eur. Ceram. Soc.* 1999, **19**, 1605–1614.
15. Wolska, E., The structure of hydrohematite. *Z. Krist.* 1981, **154**, 69–75.
16. Wolska, E. and Schwertmann, U., Nonstoichiometric structures during dehydroxylation of goethite. *Z. Krist.* 1989, **189**, 233–237.
17. Goldsztaub, S., Deshydratation des hydrates ferriques naturel. *Comptes Rendus Acad. Sci.* 1931, **193**, 533–535.
18. Watari, F., Delavignette, P., van Landuyt, J. and Amelinckx, S., Electron microscopic study of dehydration transformations. *J. Solid State Chem.* 1983, **48**, 49–64.
19. Kronberg, M. L., Plastic deformation of single crystals of sapphire: basal slip and twinning. *Acta Metall.* 1957, **5**, 507–524.
20. Löffler, L. and Mader, W., Transformation mechanism of the dehydration of diaspore. *J. Am. Ceram. Soc.* 2003, **86**, 534–540.